Published in final edited form as:
Glia. 2006 January 15; 53(2): 182–190. doi:10.1002/glia.20258.

Purinergic Receptor Antagonists Inhibit Odorant-Induced Heat Shock Protein 25 Induction in Mouse Olfactory Epithelium

Colleen C. Hegg* and **Mary T. Lucero**
Department of Physiology, University of Utah, Salt Lake City, Utah

Abstract

Heat shock proteins (HSPs) accumulate in cells exposed to a variety of physiological and environmental factors, such as heat shock, oxidative stress, toxicants, and odorants. Ischemic, stressed, and injured cells release ATP in large amounts. Our hypothesis is that noxious stimulation (in this case, strong odorant) evokes the release of ATP in the olfactory epithelium (OE). Extracellular ATP, a signal of cellular stress, induces the expression of HSPs via purinergic receptors. In the present study, in vivo odorant exposure (heptanal or R-carvone) led to a selective induction of HSP25 in glia-like sustentacular cells in the Swiss Webster mouse OE, as previously shown in rats (Carr et al., 2001). Furthermore, in vitro and in vivo administration of purinergic receptor antagonists suramin and pyridoxalphosphate-6-azophenyl-2′,4′-disulfonic acid (PPADS) blocked the expression of HSP25 immunoreactivity in sustentacular cells. ATP released by acutely injured cells could act as an early signal of cell and tissue damage, causing HSP expression and initiating a stress signaling cascade to protect against further damage. Sustentacular cells have a high capacity to detoxify xenobiotics and thereby protect the olfactory epithelium from airborne pollutants. Thus, the robust, rapid induction of HSPs in sustentacular cells may help maintain the integrity of the OE during exposure to toxicants.

Keywords

stress proteins; HSP25; ATP; sustentacular cell

INTRODUCTION

Cells respond to a wide variety of stressful stimuli, such as hypoxia, ischemia, and noxious chemical agents, by transiently increasing expression of heat shock proteins (HSPs). These proteins, defined by their physiological induction by temperature elevation (heat shock), have been found in virtually all organisms and are highly conserved phylogenetically. The major HSP families, named according to their molecular weight, include sets of proteins of ~110, 90, 70, 60, and 15–30 kDa (Fink, 1999). Constitutively expressed HSPs function as molecular chaperones and participate in protein synthesis, folding, transport and translocation under normal physiological conditions (Welch, 1992). After stress, upregulation of HSPs prevents a buildup of damaged, misfolded and aggregated proteins thus facilitating cell survival.

The small HSPs (15–30 kDa), more often found in glia (Sharp et al., 1999) than in neurons, tend to form oligomers (Arrigo et al., 1988) and have chaperone functions. HSP25 function is regulated by its degree of oligomerization and phosphorylation state (Gusev et al., 2002). In

*Correspondence to: Colleen Cosgrove Hegg, Department of Physiology, University of Utah, 410 Chipeta Way, Room 155, Salt Lake City, UT 84108-1297. c.hegg@m.cc.utah.edu.

its unphosphorylated state, HSP25 exists as large oligomers and has a chaperone function. However, stress evokes phosphorylation of HSP25, which decreases its oligomer size (Rogalla et al., 1999; Mounier and Arrigo, 2002) allowing interactions that interfere with apoptosis and specific cell death programs (Rogalla et al., 1999). Specifically, HSP25 interacts with cytochrome c preventing caspase activity (Bruey et al., 2000), and increases glutathione levels (Mehlen et al., 1996). HSP25 also associates with the microfilaments (Lavoie et al., 1993) and intermediate filaments (Nicholl and Quinlan, 1994; Salvador-Silva et al., 2001) to physiologically modulate and potentially protect and stabilize the cytoskeleton during stress.

The olfactory epithelium (OE) of mammals consists of three primary cell types: basal "progenitor" cells, glia-like sustentacular cells, and ciliated olfactory sensory neurons (Fig. 1C). Sustentacular cells function very much like glia (Okano and Takagi, 1974;Getchell, 1977) with characteristics of both the macrophage-like microglia as well as macroglia. They insulate olfactory sensory neurons both physically and chemically, (Breipohl et al., 1974), actively phagocytose dead and dying cells (Suzuki et al., 1996), and regulate the extracellular ionic environment (Breipohl et al., 1974;Rafols and Getchell, 1983). In many ways sustentacular cells are morphologically and physiologically similar to the Müller glia of the retina.

The OE is in direct contact with airborne pollutants, toxicants and microbes, and consequently is easily damaged. Although the OE exhibits a remarkable capacity for regeneration, protective mechanisms exist to minimize injury. In the OE, the sustentacular cells contain the majority of xenobiotic metabolizing enzymes which generally detoxify inhaled pollutants providing protection (Ding and Coon, 1988; Nef et al., 1989; Lazard et al., 1991). Moreover, upregulation of HSP expression in the rat OE following prolonged odorant stimuli might provide additional protection against cell death (Carr et al., 2001).

Interestingly, intracellular ATP significantly decreased when the OE was damaged by toxic fumes, presumably through release by injured cells (Kilgour et al., 2000). Thus, we tested the hypothesis that harmful stimulation (in this case, strong odorant) evokes the release of ATP and that extracellular ATP, a signal of cellular stress, induces the expression of HSPs via purinergic receptor (P2R) activation. We focused on HSP25 for two reasons: previous work in the rat showed that most cells expressing HSPs under stressful conditions were glia-like sustentacular cells (Carr et al., 2001), and recent studies indicate that most HSPs expressed in glia are members of the small HSP family (Sharp et al., 1999). We found that both in vitro and in vivo exposure of mouse OE to concentrated odorants upregulate expression of HSP25 in sustentacular cells. Furthermore, in our in vitro preparation, strong odorant causes the release of ATP. The upregulation of HSP25 expression could be inhibited by administration of P2R antagonists before odorant exposure, suggesting that both ATP release and P2R activation are involved in stress signaling in the OE. This study expands on our previous work with ATP in the olfactory system (Hegg et al., 2003) and suggests that ATP has at least two functions in the OE: modulation of the physiological response to odorants and initiation of the protective stress signaling pathway.

MATERIALS AND METHODS

Materials

All materials were purchased form Sigma-Aldrich (St. Louis, MO) unless otherwise specified.

In Vivo Experiments

All animal procedures were approved by the University of Utah Institutional Animal Care and Use Committee, and all applicable guidelines from the National Institutes of Health (NIH)

Guide for Care and Use of Laboratory Animals were followed. Odorant -induction of HSPs was performed as in Carr et al. (2001) with the following modifications. Briefly, Swiss Webster adult mice (≥25 g; Simonsen, Gilroy, CA) were injected with 100 μmol/kg suramin + pyridoxalphosphate-6-azophenyl-2′, 4′-disulfonic acid (PPADS) or an equivalent volume of mammalian Ringer's solution (in mM: 140 NaCl, 5 KCl, 1 $MgCl_2$, 2 $CaCl_2$, 10 HEPES, 10 glucose; pH 7.4; 330 mOsm). 30 min later, mice were placed in 5.5 L plastic mouse cages (11.5 × 7.5 × 5.0 in) containing 0.5 L of cornhusk pellet bedding to which 0 or 1 ml of heptanal had been added and well mixed. Cages containing odorant were kept in a hood at all times to prevent odorant exposure to control cages. The intensity of odorant was very strong; however, the odorant exposure was not harmful enough to disrupt olfactory epithelium integrity as monitored by immunohistochemistry. After 3 h of odorant exposure, mice were transferred to a fresh odorant-free cage. 6 h from the start of odorant exposure, mice were deeply anesthetized with 80 mg/kg sodium-pentobarbital (Abbott Laboratories, North Chicago, IL) and intracardial perfusion fixed with 4% paraformaldehyde (PF) in 0.1 M phosphate-buffered saline (PBS) for 15 min. This experiment was performed three separate times for each of the four conditions (with or without P2R antagonists, with or without odorants; n = 3).

Olfactory tissue was postfixed for 2 h in 4% PF, rinsed in PBS and placed in RDO-Rapid Decalcifier for 1 h (Apex Engineering Products, Aurora, IL) before dissection. Tissue was cryoprotected with sucrose, oriented in Tissue Tek OCT (Sakura Finetek, Torrance, CA) and quickly frozen. Cryostat sections (14 μm) were collected from regions shown in Figure 1A onto Superfrost Plus slides (Fisher, Pittsburgh, PA). Neonatal postnatal day 1–4 (P1–P4) mice were exposed to odorants as described above, with the exception that R-carvone was used instead of heptanal, suramin was used instead of the PPADS + suramin, and that this experiment was performed twice (n = 2) with 5 pups/condition. 6 h after the initiation of odorant exposure, neonates were decapitated, quickly dissected, and tissue was fixed by immersion in 4% PF overnight at 4°C, rinsed for 20 min in PBS and processed for immunohistochemistry as described above.

In Vitro Experiments

Coronal OE slices (300 μm) were prepared from P1–P4 mice as previously described (Hegg et al., 2003). Two slices were incubated for 2 h in each of the following solutions at 37°C in an O_2-enriched environment: Ringer's solution (control), control + 100 μM suramin, 100 μM R-carvone (Odorant), Odorant + 100 μM suramin, 10 μM ATP, 10 μM ATP + 100 μM suramin. These experiments were repeated 4 times for each of the six conditions (n = 4). Odorant treatments were performed in a separate room to prevent odorant exposure to the control slices. Tissue sections were washed 3 times and incubated in fresh Ringer's solution for an additional 4 h to allow time for the induction of HSPs. The slices were fixed in 4% PF for 1 h, rinsed and stored in PBS until immunohistochemistry was performed.

Immunohistochemistry

PF-fixed OE slices (300 μm) or cryostat sections (14 μm) were permeabilized with 0.3% Triton X-100 in PBS and blocked with 10% normal donkey serum. Primary antibodies were applied to slices or cryostat sections singly or as a mixture at 4°C overnight. Secondary antiserum was applied for 30 min (sections) or 1 h (slices) and washed in PBS. Sections were mounted in Vectashield mounting media (Vector Laboratories, Burlingame, CA) and 300-μm slices were stored in PBS. Immunoreactivity (IR) was visualized on a Zeiss confocal LSM510 argon-krypton laser scanner attached to an upright Zeiss Axioskop 2FS microscope (Zeiss, Thornwood, NY). FITC dye was excited at 488 nm and low pass filtered at 505 nm, TRITC dye was excited at 568 nm and low pass filtered at 550 nm. Control experiments included the omission of the primary antibody and omission of the secondary antibody.

Primary antibodies used were goat anti-olfactory marker protein (OMP; 1:10,000; gift from F. Margolis) and rabbit anti-HSP25 (1:750; Stressgen Biotechnologies, Victoria, BC, Canada). The HSP25 antibody recognizes the mouse orthologue of human HSP27. Secondary antibodies used were TRITC-conjugated donkey anti-goat IgG and FITC-conjugated donkey anti-rabbit IgG (1:100; Jackson ImmunoResearch Labs, West Grove, PA). All antisera were diluted in 0.3% Triton X-100 in PBS.

Quantification of In Vitro HSP Expression in OE Slices

There was reduced permeability of the antibodies through the 300-μm slices. Thus, for each OE slice, projections were created by stacking 15 confocal images taken every 8 μm in the z-axis starting from the surface from the three regions in the OE where HSP25 induction always occurs: the septum, the second endoturbinate, and the dorsal medial meatus (see Fig. 1B). Histogram counts (bin = 5 fluorescent intensity units) were made for equal areas of OE and averaged for each condition for each experimental session. The histogram counts were then normalized to the control for each experimental session and the normalized fluorescence intensity was integrated and averaged across each treatment. A 2-way ANOVA with the Bonferroni post-hoc statistical test was performed using Prism 4.1 (GraphPad Software, San Diego, CA).

Calcium Imaging

We measured intracellular calcium ($[Ca^{2+}]_i$) levels using confocal imaging of fluo-4 AM (Molecular Probes, Eugene, OR) loaded OE slices as previously described (Hegg et al., 2003). The slices were perfused continuously with Ringer's solution with 500 μM probenecid (to prevent fluo-4 AM dye efflux) at a flow rate of 1.5–2.0 ml/min. Test solutions were applied by bath exchange with a 200-μl loop injector. The Zeiss confocal system described above was used for data acquisition and analysis. The transmission at 488 nm was less than 5% of the total laser power (25 mW). Fluorescent emission was longpass filtered at 510 nm. Time series experiments collected 1400 × 700 pixel images at 0.5 Hz. Traces were baseline corrected by subtracting a linear fit to the first 20 s of recording and normalized as the change in fluorescence intensity/the maximum fluorescence intensity of 255 and multiplied by 100 (% ΔF/F).

Bioluminescence Detection of ATP Released From Olfactory Epithelium Slices

ATP was quantified using 0.5 mM D-luciferin and 4 μg/ml luciferase in Ringer's solution obtained from an ATP determination kit (Molecular Probes, Eugene, OR). Bioluminescence, in relative light units, was recorded continuously with 1-s photon collection intervals using a Turner TD20/20^n luminometer. Standard curves of ATP (Mg salt) were performed daily by serial dilution from a 0.5 M ATP stock. Two OE slices (500 μm) were simultaneously placed in the luciferin and luciferase solution and basal release rates measured. Once basal release was stabilized (~20 min), a bolus of either Ringer's (control) or R-carvone was administered (100 μM final concentration) and ATP release monitored. At the end of an experiment, a bolus of Triton X-100 was added (0.5% final concentration) to lyse the cells and determine total ATP.

RESULTS

Odorant Exposure Induces HSP25 Expression in Sustentacular Cells of the Neonatal Mouse

Initially, we verified odorant-evoked HSP expression in sustentacular cells in neonatal mouse olfactory epithelium (OE). Three areas of the nasal cavity were examined for HSP25 expression (Fig. 1A,B). Expression of odorant-induced HSP25 occurred only in the regions indicated in Figure 1B (green lines). Odorant evoked HSP25 expression was strongest in the sustentacular cells; there was no colocalization between HSP25 and OMP, a marker for mature olfactory

receptor neurons (ORNs) along the entire length of ORNs (Fig. 1D). The odorant-induced HSP expression was observed throughout the cytoplasm of the sustentacular cell, from the elongated cell soma at the epithelial surface to the central stalk that extends to the basement membrane where it ends in an endfoot process. As there is strong expression of HSP25 in both the central stalk and the endfoot process, we conclude that HSP25 IR near the basal lamina is in the endfoot process, although we cannot eliminate the possibility that basal cells also express HSP25. In contrast, in control (no odorant) animals, HSP25 IR was infrequently observed primarily in the basal cell layer of the OE, most likely in the sustentacular cell endfoot processes, although we cannot exclude the possibility that basal cells constitutively express HSP25 (Fig. 1E,E′). There was no constitutive HSP25 IR observed in the respiratory epithelium (data not shown).

Odorant-induced HSP25 IR in sustentacular cells was observed in the OE of the nasal septum (Fig. 1D), the dorsal medial meatus (Fig. 1F), the second endoturbinate (Fig. 1G), the second ectoturbinate (Fig. 1H), the third endoturbinate (Fig. 1J), and the fourth endoturbinate (data not shown). Note that portions of the second– fourth endoturbinates had weak odorant-induced HSP25 IR (dashed green line Fig. 1B,J). HSP25 IR was also observed after odorant exposure in respiratory epithelium located in the dorsal lateral meatus (Fig. 1I,I′), the lateral aspects of the second endo- and ectoturbinates (Fig. 1G,H), the nasoturbinates (Fig. 1K), and the maxilloturbinates (Fig. 1K). Olfactory ensheathing cells (OECs) ensheathe the ORN axons into nerve bundles when they leave the OE on the way to the olfactory bulb. Odorant-induced HSP25 IR occurred in OECs surrounding the nerve bundles in the lamina propria (Fig. 1I,I′) and in nerve bundles adjacent to the olfactory nerve layer of the olfactory bulb (Fig. 1L,L′).

Odorant and Purinergic Receptor Agonist Exposure Induces HSP25 Expression In Vitro

We next tested the hypothesis that ATP and P2R activation are involved in odorant-induced HSP induction. Neonatal mouse OE slices incubated in either 100 μM odorant ($_R$-carvone) or 10 μM ATP for 2 h had robust increases in HSP25 expression throughout the cytoplasm of sustentacular cells (Fig. 2A – C). HSP25 IR was significantly greater in both the ATP and odorant treated slices as compared with control treated slices ($P < 0.001$, n = 4; Fig. 2G). Thus, both odorant and exogenous ATP evoked HSP25 upregulation in an in vitro OE slice preparation.

P2R Antagonism Inhibits Odorant and Purinergic Agonist-Induced HSP25 Upregulation

We previously reported that sustentacular cells express G-protein coupled P2Y purinergic receptors (Hegg et al., 2003) and that they respond to P2R agonists ATP and UTP with increases in $[Ca^{2+}]_i$. To determine whether P2R activation was involved in HSP25 induction we incubated slices in either odorant or ATP in the presence of 100 μM suramin, a general P2R antagonist. This concentration of suramin blocks both ATP and UTP evoked Ca^{2+} transients in sustentacular cells as well as ORNs in our OE slice preparation (Fig. 3). Although suramin did not have a significant effect on the level of HSP25 expression in control treated slices (Fig. 2A,D,G), we observed that suramin significantly inhibited the ATP-evoked induction of HSP25 in sustentacular cells ($P < 0.001$, n = 4; Fig. 2B,E,G). This suggests that ATP-induced HSP25 expression is mediated in part by activation of P2Rs. Moreover, we observed that suramin significantly inhibited the odorant-evoked induction of HSP25 in sustentacular cells ($P < 0.001$, n = 4; Fig. 2C,F,G) suggesting that strong odorant stimulation releases ATP, which activates P2Rs and induces the expression of HSP25.

In Vitro Odorant Exposure Stimulates ATP Release

We measured real-time ATP release from OE slices. When we initially transferred the slices into the luminometer, ATP levels were elevated, most likely from mechanical stimulation and subsequent ATP release. However, the concentration of ATP decayed with apparent first-order kinetics (data not shown), presumably resulting from endogenous ecto-nucleotidase hydrolysis

of ATP. The ATP levels eventually stabilized and persisted at nanomolar concentration (Fig. 4). This could either represent sustained cell lysis due to the in vitro preparation, or tonic basal release of ATP. Previous reports show that various types of resting cells constitutively release ATP at a rate that equals steady state ATP hydrolysis (Lazarowski et al., 2000). In the presence of 100 μM R-carvone we observed a delayed increase in ATP in four of five experiments (Fig. 4). Peak ATP levels reached 414 ± 235 relative light units (mean ± SEM; n = 4) corresponding to a 3.0 ± 1.2 fold increase (mean ± SEM; n = 4) in ATP release. When Ringer's solution was applied instead of odorant there was no increase in ATP release (Fig. 4). Thus, odorants, at the same concentration that upregulated HSP25 expression, induce ATP release.

In Vivo Odorant Exposure Upregulates HSP25 Expression Via P2R Activation

Finally, we sought to verify that odorant exposure evokes ATP release, P2R activation, and HSP25 induction in whole animals. Either suramin alone (100 mmol/ kg) for the neonates, P2R antagonists (100 mmol/kg suramin and PPADS) for the adults, or an equivalent volume of Ringer's solution was pre-administered before exposure to odorant (R-carvone for the neonates and heptanal for the adults). We found that in the Ringer's solution-injected mice, in vivo odorant exposure led to specific induction of HSP25 in sustentacular cells as compared with control (no odorant exposure) (Fig. 5A – D). Pre-administration of P2R antagonists to control mice (no odorant exposure) did not affect HSP25 expression as compared with Ringer's solution-injected control mice (Fig. 5A,B vs. G,H). However, P2R antagonist administration effectively blocked the odorant-evoked expression of HSP25 (Fig. 5E,F). Thus, induction of HSP25 expression by strong odorant can be prevented by in vivo administration of P2R antagonists.

DISCUSSION

We have examined the effects of noxious concentrations of odorants on HSP induction in a mouse model. We observed upregulation of HSP25 in both neonatal and adult sustentacular cells following odorant exposure, a result that was not surprising as similar upregulation of the HSP25 has been reported in the adult rat (Carr et al., 2001). HSP25 induction also occurred after exposure to extracellular ATP in neonatal OE slices. The increased expression of HSP25 in sustentacular cells could be blocked by administration of P2R antagonists before odorant exposure, suggesting that activation of P2Rs plays an important role in the stress response in the OE. Although suramin and PPADS have other systemic functions, such as an antifibrotic or anti-apoptotic agent, in general both are functionally selective antagonists for the P2 class of purinergic receptors (Ralevic and Burnstock, 1998).

It is generally thought that denatured proteins serve as a stimulus for induction of HSPs (Morimoto, 1998). Our results indicate that during odorant-evoked HSP25 expression, activation of P2Rs is also required. Even minor lesions to the cell membrane would be expected to drive significant efflux of ATP, given the large (mM) gradient in ATP concentration between the intracellular and extracellular milieu. ATP released by acutely injured cells could act in an autocrine or paracrine way to activate P2Rs and signal cell and tissue damage, causing protective HSP25 expression. There are two subtypes of P2Rs: P2Y G-protein coupled receptors or P2X ion channel-forming receptors. Through either of these P2R subtypes, ATP is able to stimulate an increase in $[Ca^{2+}]_i$ (Hegg et al., 2003). Thus, a Ca^{2+}-dependent cascade of intracellular events could trigger HSP25 induction. A number of HSPs are constitutively or inductively expressed in the CNS and their upregulation and presence has been connected to protection of neurons and glia (Mehlen et al., 1999; Benn et al., 2002).

In the OE, P2X receptors are located on the ORNs and P2Y receptors are located on both the sustentacular cells and the olfactory receptor neurons (Hegg et al., 2003). In the present study as well as in all studies examining the expression of stress-induced HSPs in the OE (Kilgour

et al., 2000; Carr et al., 2001, 2004; Simpson et al., 2004, 2005), the predominant cell type exhibiting HSP upregulation was the sustentacular cell. This observation is surprising given our hypothesis of a P2R role in HSP induction, as P2Rs are present on both ORNs and sustentacular cells. However, there are many possible explanations for this apparent discrepancy. The sustentacular cell, with the cell soma located in the upper third of the OE, is positioned to receive direct interaction with inhaled toxicants. Moreover, sustentacular cells contain the xenobiotic metabolizing enzymes for the OE (Ding and Coon, 1988; Nef et al., 1989; Lazard et al., 1991). Thus, sustentacular cells endure more stresses than ORNs and are more easily damaged by both inhaled toxicants and systemic compounds that can be metabolized into toxicants. Finally, the small HSPs are predominantly expressed in glia as opposed to neurons (Sharp et al., 1999), and in the mouse OE, we did not observe HSP25 immunoreactivity in ORNs under any conditions. In support of our hypothesis for a purinergic role in HSP25 induction, we observed that strong odorant stimulated a 3-fold increase in ATP release from OE slices in vitro. Moreover, heat shock and toxic chemicals caused a reduction in intracellular ATP levels in a rat nasal explant culture system that was concurrent with an increase in HSP70 (Simpson et al., 2004, 2005).

Expression and Function of HSPs in the Olfactory System

HSPs have been insufficiently examined in the olfactory system with the majority of studies concentrating on the HSP70 family. In general, HSP70 is expressed in the supranuclear region of sustentacular cells, basal cells, and Bowman's glands and in a scattered subpopulation of olfactory receptor neurons of the "unstressed" rat (Carr et al., 2001; Simpson et al., 2004). Based on the striking induction of HSPs predominantly in sustentacular cells, we focused our investigation on HSP25, a member of the small HSP family that is expressed largely in glia (Sharp et al., 1999). In the present study, the only expression of HSP25 in the "unstressed" mouse was observed in the basal cell layer of the neonate, although we could not determine whether HSP25 IR was in the basal cells or sustentacular cell endfoot processes. Interestingly, constitutive expression of HSP25 in the basal cell layer disappears by adulthood in mice. The absence of HSP25 expression in adult mice is different from the observed expression of HSP25 in the basal cells of the adult rat (Carr et al., 2001). However, "constitutive" expression of an inducible HSP like HSP25 could be residual expression from a previous stress episode.

HSPs are important players in development and growth (Christians et al., 2003). In the CNS, HSPs are differentially regulated during neuronal maturation and appear to have a role in neuronal differentiation (Calabrese et al., 2002). In the olfactory system, in an immortalized rat olfactory progenitor cell line, HSP27 induction is correlated to neuronal differentiation and escape from apoptosis (Mehlen et al., 1999). Thus, expression of HSP25 in the basal cell layer of the mouse OE, where the OE progenitors reside, suggests a role for HSP25 in cell differentiation and proliferation in the neonatal olfactory system.

Upon various stresses including heat shock (Carr et al., 2001; Simpson et al., 2004), anesthetics (Carr and Farbman, 1993), or odorant exposure (Carr et al., 2001), HSP70 is upregulated in the adult rat primarily in sustentacular cells, similar to observations in our studies of odorant-evoked expression of HSP25 in mouse sustentacular cells. One striking difference between HSP25 and HSP70 in the sustentacular cell of both rats and mice is its cellular localization. HSP70 was expressed in the supranuclear region of the sustentacular cell (Carr et al., 2001; Simpson et al., 2004), in close proximity to the endoplasmic reticulum, suggesting a role as a molecular chaperone to facilitate protein folding. In contrast, in this study and in an earlier report (Carr et al., 2001) odorant-evoked HSP25 expression occurred throughout the cytoplasm of the sustentacular cell, suggesting an additional role for HSP25 in the OE. Given that small HSPs stabilize the cytoskeleton (Lavoie et al., 1993; Nicholl and Quinlan, 1994; Salvador-Silva et al., 2001), odorant-induced HSP25 expression throughout the cytoplasm and in basal

processes suggests that HSP25 interacts with components of the cytoskeleton to help maintain cytoskeletal integrity (Carr et al., 2001). HSP25, in addition to having a role as chaperone, may inhibit apoptosis thereby promoting cell survival (Mehlen et al., 1999; Bruey et al., 2000; Garrido et al., 2001; Concannon et al., 2003). Clearly, both the function of various HSPs and the differences in HSP expression in the olfactory epithelium between species and across different ages need to be delineated.

Purinergic receptors appear to play an integral role in signaling acute damage in the olfactory epithelium. Damaged cells release ATP, thereby activating purinergic receptors on neighboring sustentacular cells, ORNs and basal cells, and initiating a stress signaling cascade involving HSPs for neuroprotection.

Acknowledgments

The authors thank Sam Victor, Ja Thammanavong, and Kathleen Davis for technical assistance. This research was supported by NIH NIDCD grants DC004953 and DC006897 (to C.C.H.) and by NINDS grants NS07938 and NIDCD DC02994 (to M.T.L.).

Grant sponsor: National Institutes of Health, National Institute on Deafness and Other Communication Disorders (NIDCD); Grant number: DC004953; Grant number: DC006897; Grant number: DC002994; Grant sponsor: National Institute of Neurological Disorders and Stroke; Grant number: NS07938.

REFERENCES

Arrigo AP, Suhan JP, Welch WJ. Dynamic changes in the structure and intracellular locale of the mammalian low-molecular-weight heat shock protein. Mol Cell Biol 1988;8:5059–5071. [PubMed: 3072471]

Benn SC, Perrelet D, Kato AC, Scholz J, Decosterd I, Mannion RJ, Bakowska JC, Woolf CJ. Hsp27 upregulation and phosphorylation is required for injured sensory and motor neuron survival. Neuron 2002;36:45–56. [PubMed: 12367505]

Breipohl W, Laugwitz HJ, Bornfeld N. Topological relations between the dendrites of olfactory sensory cells and sustentacular cells in different vertebrates. An ultrastructural study. J Anat 1974;117:89–94. [PubMed: 4844653]

Bruey JM, Ducasse C, Bonniaud P, Ravagnan L, Susin SA, az-Latoud C, Gurbuxani S, Arrigo AP, Kroemer G, Solary E, Garrido C. Hsp27 negatively regulates cell death by interacting with cytochrome c. Nat Cell Biol 2000;2:645–652. [PubMed: 10980706]

Calabrese V, Scapagnini G, Ravagna A, Giuffrida Stella AM, Butterfield DA. Molecular chaperones and their roles in neural cell differentiation. Dev Neurosci 2002;24:1–13. [PubMed: 12145406]

Carr VM, Farbman AI. Effect of ketamine on stress protein immunoreactivities in rat olfactory mucosa. NeuroReport 1993;5:197–200. [PubMed: 8298074]

Carr VM, Menco BP, Yankova MP, Morimoto RI, Farbman AI. Odorants as cell-type specific activators of a heat shock response in the rat olfactory mucosa. J Comp Neurol 2001;432:425–439. [PubMed: 11268007]

Carr VM, Ring G, Youngentob SL, Schwob JE, Farbman AI. Altered epithelial density and expansion of bulbar projections of a discrete HSP70 immunoreactive subpopulation of rat olfactory receptor neurons in reconstituting olfactory epithelium following exposure to methyl bromide. J Comp Neurol 2004;469:475–493. [PubMed: 14755530]

Christians ES, Zhou Q, Renard J, Benjamin IJ. Heat shock proteins in mammalian development. Semin Cell Dev Biol 2003;14:283–290. [PubMed: 14986858]

Concannon CG, Gorman AM, Samali A. On the role of Hsp27 in regulating apoptosis. Apoptosis 2003;8:61–70. [PubMed: 12510153]

Ding X, Coon MJ. Purification and characterization of two unique forms of cytochrome P-450 from rabbit nasal microsomes. Biochemistry 1988;27:8330–8337. [PubMed: 3242590]

Fink AL. Chaperone-mediated protein folding. Physiol Rev 1999;79:425–449. [PubMed: 10221986]

Garrido C, Gurbuxani S, Ravagnan L, Kroemer G. Heat shock proteins: endogenous modulators of apoptotic cell death. Biochem Biophys Res Commun 2001;286:433–442. [PubMed: 11511077]

Getchell TV. Analysis of intracellular recordings from salamander olfactory epithelium. Brain Res 1977;123:275–286. [PubMed: 66084]

Gusev NB, Bogatcheva NV, Marston SB. Structure and properties of small heat shock proteins (sHsp) and their interaction with cytoskeleton proteins. Biochemistry (Mosc) 2002;67:511–519. [PubMed: 12059769]

Hegg CC, Greenwood D, Huang W, Han P, Lucero MT. Activation of purinergic receptor subtypes modulates odor sensitivity. J Neurosci 2003;23:8291–8301. [PubMed: 12967991]

Kilgour JD, Simpson SA, Alexander DJ, Reed CJ. A rat nasal epithelial model for predicting upper respiratory tract toxicity: in vivo–in vitro correlations. Toxicology 2000;145:39–49. [PubMed: 10771130]

Lavoie JN, Hickey E, Weber LA, Landry J. Modulation of actin microfilament dynamics and fluid phase pinocytosis by phosphorylation of heat shock protein 27. J Biol Chem 1993;268:24210–24214. [PubMed: 8226968]

Lazard D, Zupko K, Poria Y, Nef P, Lazarovits J, Horn S, Khen M, Lancet D. Odorant signal termination by olfactory UDP glucuronosyl transferase. Nature 1991;349:790–793. [PubMed: 1900353]

Lazarowski ER, Boucher RC, Harden TK. Constitutive release of ATP and evidence for major contribution of ecto-nucleotide pyrophosphatase and nucleoside diphosphokinase to extracellular nucleotide concentrations. J Biol Chem 2000;275:31061–31068. [PubMed: 10913128]

Mehlen P, Coronas V, Ljubic-Thibal V, Ducasse C, Granger L, Jourdan F, Arrigo AP. Small stress protein Hsp27 accumulation during dopamine-mediated differentiation of rat olfactory neurons counteracts apoptosis. Cell Death Differ 1999;6:227–233. [PubMed: 10200573]

Mehlen P, Kretz-Remy C, Preville X, Arrigo AP. Human hsp27, Drosophila hsp27 and human alphaB-crystallin expression-mediated increase in glutathione is essential for the protective activity of these proteins against TNFalpha-induced cell death. EMBO J 1996;15:2695–2706. [PubMed: 8654367]

Morimoto RI. Regulation of the heat shock transcriptional response: cross talk between a family of heat shock factors, molecular chaperones, and negative regulators. Genes Dev 1998;12:3788–3796. [PubMed: 9869631]

Mounier N, Arrigo AP. Actin cytoskeleton and small heat shock proteins: how do they interact? Cell Stress Chaperones 2002;7:167–176. [PubMed: 12380684]

Nef P, Heldman J, Lazard D, Margalit T, Jaye M, Hanukoglu I, Lancet D. Olfactory-specific cytochrome P-450. cDNA cloning of a novel neuroepithelial enzyme possibly involved in chemoreception. J Biol Chem 1989;264:6780–6785. [PubMed: 2708343]

Nicholl ID, Quinlan RA. Chaperone activity of alpha-crystallins modulates intermediate filament assembly. EMBO J 1994;13:945–953. [PubMed: 7906647]

Okano M, Takagi SF. Secretion and electrogenesis of the supporting cell in the olfactory epithelium. J Physiol Lond 1974;242:353–370. [PubMed: 4549073]

Rafols JA, Getchell TV. Morphological relations between the receptor neurons, sustentacular cells and Schwann cells in the olfactory mucosa of the salamander. Anat Rec 1983;206:87–101. [PubMed: 6881554]

Ralevic V, Burnstock G. Receptors for purines and pyrimidines. Pharmacol Rev 1998;50:413–492. [PubMed: 9755289]

Rogalla T, Ehrnsperger M, Preville X, Kotlyarov A, Lutsch G, Ducasse C, Paul C, Wieske M, Arrigo AP, Buchner J, Gaestel M. Regulation of Hsp27 oligomerization, chaperone function, and protective activity against oxidative stress/tumor necrosis factor alpha by phosphorylation. J Biol Chem 1999;274:18947–18956. [PubMed: 10383393]

Salvador-Silva M, Ricard CS, Agapova OA, Yang P, Hernandez MR. Expression of small heat shock proteins and intermediate filaments in the human optic nerve head astrocytes exposed to elevated hydrostatic pressure in vitro. J Neurosci Res 2001;66:59–73. [PubMed: 11599002]

Sharp FR, Massa SM, Swanson RA. Heat-shock protein protection. Trends Neurosci 1999;22:97–99. [PubMed: 10199631]

Simpson SA, Alexander DJ, Reed CJ. Heat shock protein 70 in the rat nasal cavity: localisation and response to hyperthermia. Arch Toxicol 2004;78:344–350. [PubMed: 15007540]

Simpson SA, Alexander DJ, Reed CJ. Induction of heat shock protein 70 in rat olfactory epithelium by toxic chemicals: in vitro and in vivo studies. Arch Toxicol 2005;79:224–230. [PubMed: 15690153]

Suzuki Y, Takeda M, Farbman AI. Supporting cells as phagocytes in the olfactory epithelium after bulbectomy. J Comp Neurol 1996;376:509–517. [PubMed: 8978466]

Welch WJ. Mammalian stress response: cell physiology, structure/ function of stress proteins, and implications for medicine and disease. Physiol Rev 1992;72:1063–1081. [PubMed: 1438579]

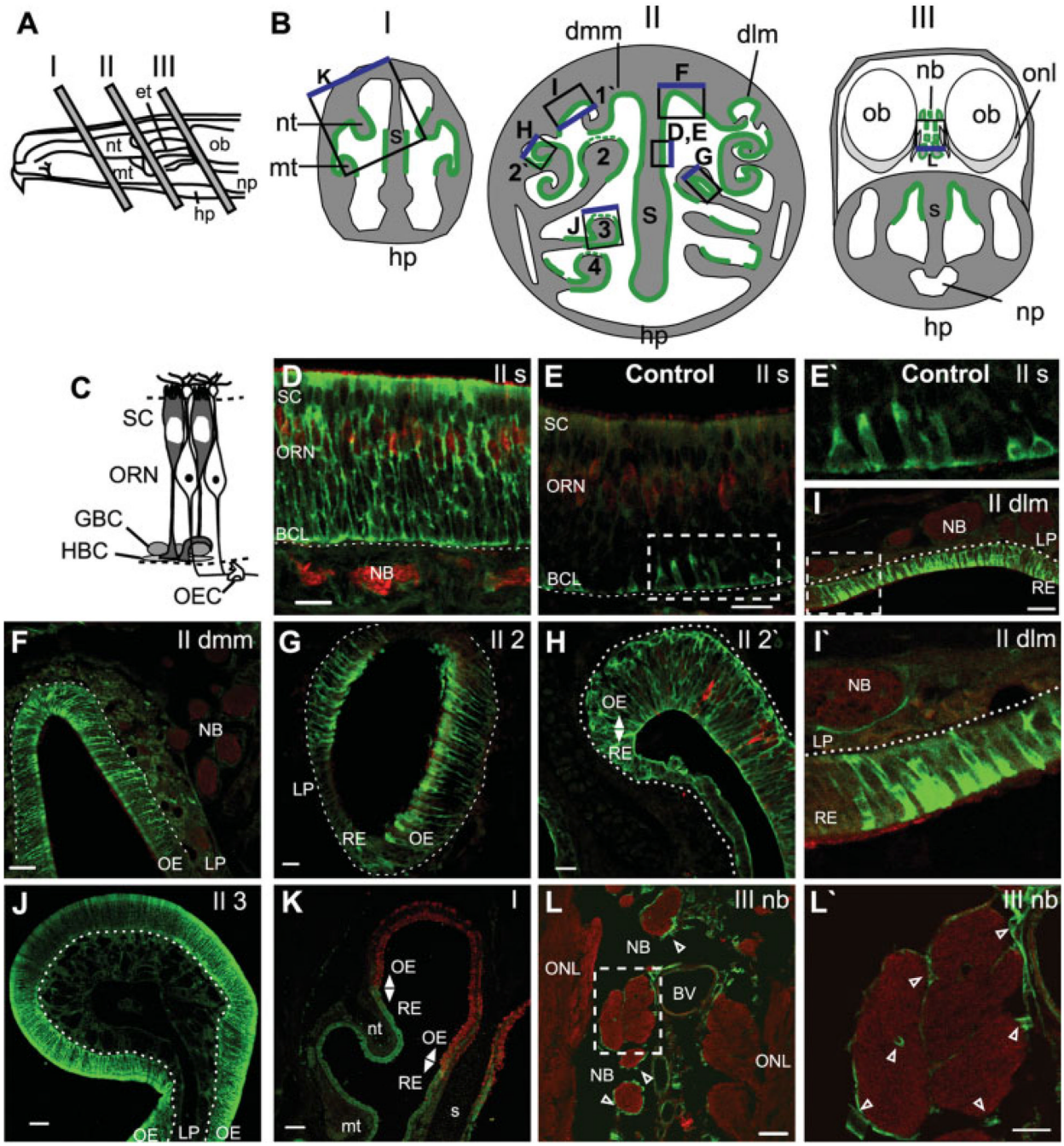

Fig. 1.

In vivo odorant exposure evokes HSP25 expression in neonatal mouse olfactory epithelium. **A:** Exposed lateral wall of the rodent nasal airway showing locations of tissue selected for analysis. **B:** Schematics of the anterior face of tissue blocks depicted in A. Regions of odorant-induced HSP25 IR are shown in green, with regions of weak IR depicted by dashed green lines. The boxes indicate regions shown in D–L, and the blue edge orients to the top of each image. The two sides in BII depict tissue blocks from slightly different levels. Drawings are not to scale. **C:** Schematic of the olfactory epithelium. **D**–**L**′: Neonatal Swiss Webster mice were exposed to no odorant (control, **E,E**′) or R-carvone (**D,F**–L′) as described in Methods. All tissue was labeled with anti-HSP25 (green), and **D–I,K,L** were also labeled with anti-olfactory

marker protein (OMP; red). E′,I′,L′, enlargements of the boxes in E,I,L. Dashed white lines indicate basement membrane. Open arrowheads indicate OECs. Nt, nasoturbinate; mt, maxilloturbinate; et, ethmoids; hp, hard palate; np, nasopharynx; ob, olfactory bulb; S, septum; dlm, dorsal lateral meatus; dmm, dorsal medial meatus; 1′-2′, first–second ectoturbinates; 2–4, second–fourth endoturbinates; onl, olfactory nerve layer; t, turbinate, nb, nerve bundle; SC, sustentacular cell layer; ORN, olfactory receptor neuron layer; HBC, horizontal basal cell; GBC, globose basal cell; OEC, olfactory ensheathing cell; OE, olfactory epithelium; RE, respiratory epithelium; BCL, basal cell layer; LP, lamina propria. Scale bars = 100 μm in K; 50 μm in F,J; 20 μm in D,E,G–I,L,L′).

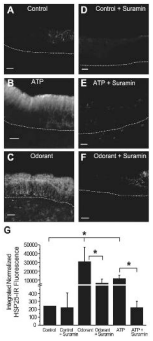

Fig. 2.

In vitro exposure to ATP and odorant causes upregulation of HSP25 that is inhibited by a P2R antagonist. **A**–**F:** Projections of HSP25 IR created by stacking 15 confocal images taken every 8 μm in the z-axis. Dashed lines indicate basement membrane. **G:** Integrated normalized HSP25 IR fluorescence for each treatment group (n = 4). **P* < 0.001. Scale bars = 20 μm in A,B,D,E; 50 μm in C,F.

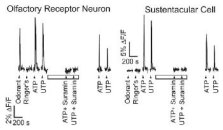

Fig. 3.

Effects of P2R agonists and antagonists on $[Ca^{2+}]_i$ levels. Fluorescence increases measured from an individual ORN and a sustentacular cell in a fluo-4 AM loaded mouse OE slice. R-Carvone (10 μM; odorant), Ringer's solution, and P2R agonists ATP and UTP (10 μM) were superfused onto the slice at times indicated by triangles. Slices were exposed to suramin (100 μM, open bar), a P2R antagonist, 5 min before purinergic agonist superfusion.

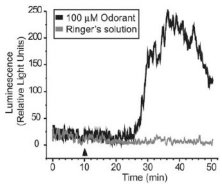

Fig. 4.

ATP is released from OE slices after odorant exposure. Raw ATP bioluminescence data from two separate experiments performed on the same day. Odorant (100 µM final concentration; black line) or Ringer's solution (gray line) was applied after 10 min (arrowhead) of recording steady state basal ATP release.

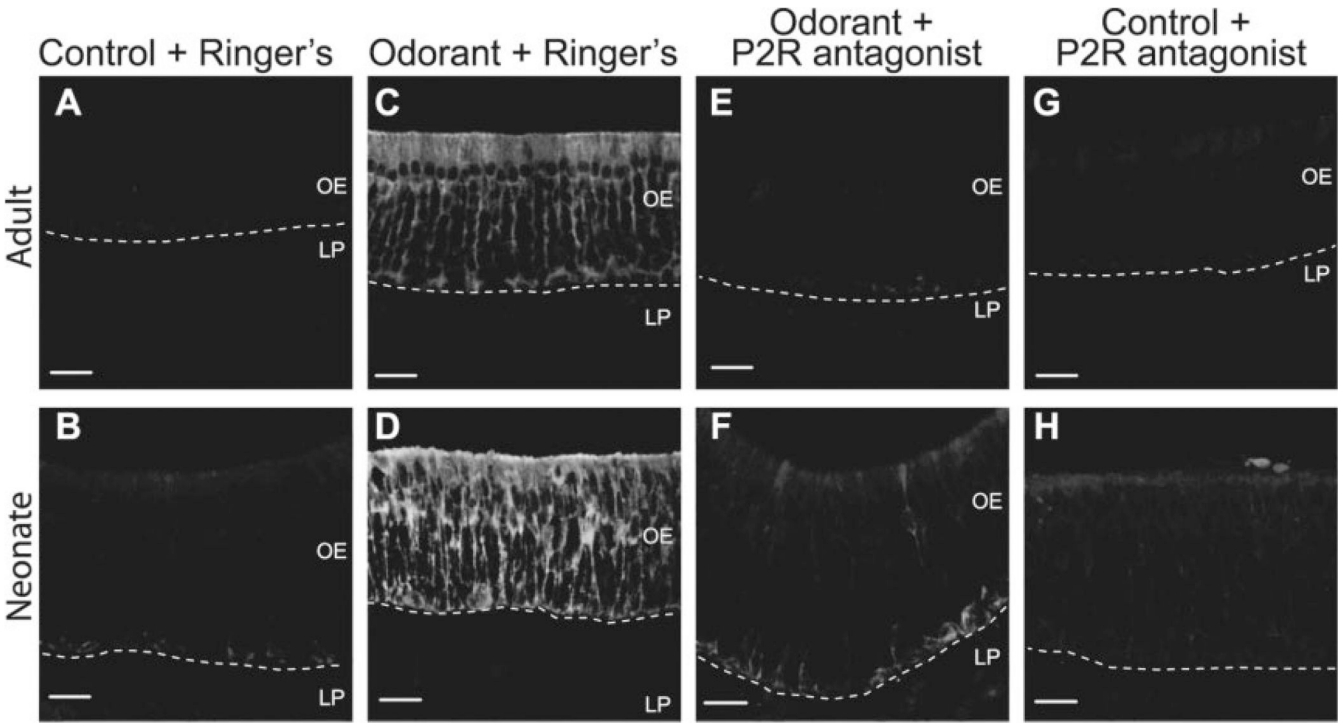

Fig. 5.

Administration of P2R antagonists inhibits odorant-evoked expression of HSP25 in vivo. 3-h exposure to odorant caused HSP25 upregulation in both adult (**C**) and neonatal (**D**) sustentacular cells as compared with control adults (**A**) and neonates (**B**). Pre-administration of P2R antagonists inhibits the odorant-induced expression of HSP25 in adults (**E**) and neonates (**F**), but does not affect HSP25 expression in control adults (**G**) or neonates (**H**). B,D,F,H: Projections of 20 confocal images taken every 0.89 μm in the z-axis. Dashed lines indicate basement membrane. LP, lamina propria; OE, olfactory epithelium. Scale bars = 20 μm.